Determining Natural and Accessible Gestures using Uncontrolled Manifolds and Cybernetics

Hairong Jiang, *Student Member, IEEE*, Chun-Hao Hsu, Bradley S. Duerstock, *Member, IEEE*, Juan P. Wachs, *Member, IEEE*

Abstract— **Recent studies revealed that hand gesture-based interfaces can complement therapies for individuals with upper motor impairments and reduce the need of traditional rehabilitation sessions through hospital visits. Unfortunately, existing gesture-based interfaces have been developed without considering the physical limitations of users with motor impairments. An analytic approach was presented in our previous work to convert existing gesture-based interfaces designed for able-bodied individuals to be usable by individuals with quadriplegia using the Laban Theory of Movement. This paper extends the previous work by including gesture variability analysis (based on Uncontrolled Manifolds theory) and robotic execution. A WAM robotic arm was used to mimic gesture trajectories and a physical metric was empirically obtained to evaluate the physical effort of each gesture. At last, an integration method was presented to determine the accessible gesture set based on both the stability and empirical robot execution. For all the gesture classes, the accessible gestures were found to lie within 31% of the optimality of stability and work, respectively.**

I. Introduction

Hand gestures have become an effective control modality for human computer interaction (HCI) leveraging on the quick growth of 3D optical sensors (i.e. Kinect® and Leap motion) [1] and accelerometers armband [2]. Recent studies indicate that playing exergames can benefit users with upper motor impairments, since gesture commands can complement users' hands-off physical therapy [3], [4]. Unfortunately, commercial gesture-based consoles are developed without considering the physical constraints of users with motor impairments, neither their operational needs. Thus, there is a paradox: the same technologies that are usable to rehabilitate patients, cannot be accessed by those patients due to the very nature of their design.

While assistive technologies (AT) and rehabilitation engineering have allocated major scientific and applied efforts to design gesture-based interfaces for individuals with disabilities for activities of daily living (ADL) [5], currently there is no generalizable solution to convert standard gestures to those usable for individuals with motor impairments. The question of determining the optimal gesture sets usable for individuals with disabilities is an open research question.

Related work leveraged on two approaches to determine optimal gesture sets for touchless interfaces: technology-based approach [6] and human-based approach [7]. The objective of the technology-based approach is to select a gesture set that can facilitate system implementation [8], [9] To the contrary, the human-based approach determines gesture sets based on studying the usability of the interaction between users and automated systems [10], [11]. Previous research also considered the integration of human and technical approach together [12], [13].

Regardless of the approach used to determine the gesture sets, either technology driven, user driven or hybrid, objective metrics can be applied to those selections [14]. For example, variability is an important objective metric to examine the mechanisms of human motor systems and evaluate human performance [15]. The Uncontrolled Manifold (UCM) framework provides a strategy to deal with redundant systems of human motion and was applied to analyze this variability [16]. It was first presented by Scholz and Schöner [17] in a targeting task using a multi-joint limb and the joints have more DOFs than the hand. In that work, the UCM was applied to analyze the effect of variability on the pointing constancy. The UCM theory assumes that the task redundant space is structured according to the task [18], and was applied to test the stability of the task variables. The variability of the control variables (i.e. the joint configurations) can be decomposed into a component that lies within a manifold that does not affect the task variable (the UCM) and a perpendicular component that affects the task variable. Nisky and her colleagues [19] tested the stability of a task using a ratio between the variability that lies within the UCM and the variability that lies perpendicular to it. The task variable (using a set of control variables) was defined to be stabilized if the ratio is greater than one [20].

Our previous work [21] presented a methodology that analytically and automatically project existing patterns of gestural behavior to match those of users with motor impairments and to make commercial gestural technologies accessible to users with physical impairments. An automatic gesture projection approach concerning physical limitations was presented to provide usable and effective candidate gestures for users with quadriplegia. A subjective method was used to determine the final gesture set from candidate gestures.

*This research was supported by Purdue Research Foundation Grant and the National Institute of Health Director's ARRA Pathfinder Award to Promote Diversity in the Scientific Workplace (1DP4GM096842-01).

H. Jiang, is with School of Industrial Engineering, Purdue University, West Lafayette, IN 47907 USA (e-mail: jiang115@ purdue.edu).

C. Hsu, is with Purdue University, West Lafayette, IN 47907 USA. (e-mail: hsu92@purdue.edu).

B. S. Duerstock, is with the School of Industrial Engineering and Weldon School of Biomedical Engineering, Purdue University, West Lafayette, IN 47907, (e-mail: bsd@purdue.edu).

J. P. Wachs, is with the School of Industrial Engineering, Purdue University, West Lafayette, IN 47907, (corresponding author, phone:765-496-7380; e-mail: jpwachs@purdue.edu).

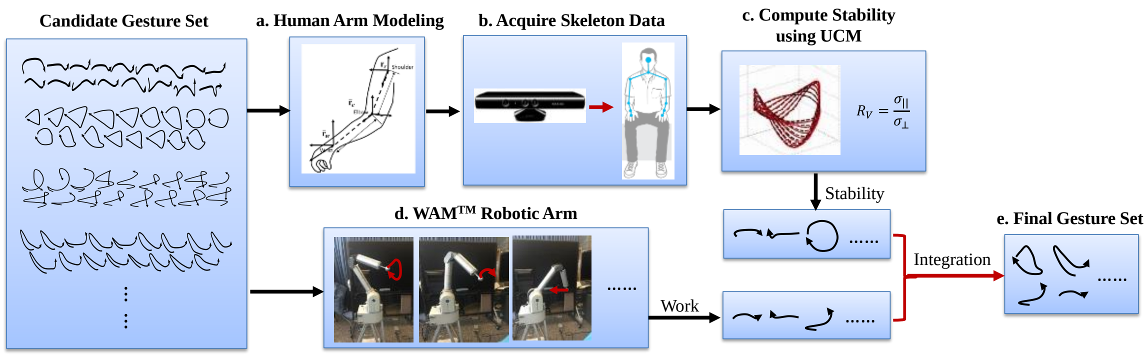

Figure 1. System Architecture

This paper proposes three main contributions: (1) an analytic approach to analyze human arm variability based on the UCM framework and evaluates gestures based on the concept of stability; (2) simulate the constrained gestures using a WAM™ robotic arm and present a metric to estimate *work* exhorted gestures' physical work; and (3) integrate stability and work to determine the final accessible gesture set.

II. Brief Introduction of Previous Work

A. Problem Definition

Our previous work [21] addressed the problem of "how to project standard gestures from a known manifold to a constrained (unknown) manifold that corresponds to the space where people with upper motor impairments use". We provide here a short summary of our previously developed method to put this work in context. Refer to [21] for more details of this theory. Let $\boldsymbol{G}$ denote a standard lexicon with N gestures and $\widetilde{\boldsymbol{G}}$ represent a constrained gesture lexicon corresponding to those gestures in $\boldsymbol{G}$. g_n and $\tilde{g}_n$ ($n = 1,2,\dots,N$) denote the nth gesture in $\boldsymbol{G}$ and $\widetilde{\boldsymbol{G}}$, respectively (Eq. 1 and 2). Let $\mathcal{L}$ denote a mapping from a gesture trajectory to a feature vector, and $\breve{g}$ be a random gesture trajectory. $\boldsymbol{\Psi}$ denotes a set of pre-trained transform functions that maps the feature vector of a standard gesture to a set of feature vectors that correspond to constrained gestures. The problem is presented as: finding a constrained gesture lexicon to satisfy Eq. 3 and 4 (Figure 2).

$$\boldsymbol{G} = \{g_1, g_2, \dots, g_n, \dots, g_N\} \quad (n = 1,2,\dots,N) \tag{1}$$

$$\widetilde{\boldsymbol{G}} = \{\tilde{g}_1, \tilde{g}_2, \dots, \tilde{g}_n, \dots, \tilde{g}_N\} \quad (n = 1,2,\dots,N) \tag{2}$$

$$\tilde{g}_n = \arg\min_{\breve{g}} \|\mathcal{L}(\breve{g}) - \boldsymbol{\Psi}(\mathcal{L}(g_n))\| \tag{3}$$

$$\text{s.t. } n \le N, n \in \mathbb{Z}^+, g_n \in \boldsymbol{G}, \text{ and } \tilde{g}_n \in \widetilde{\boldsymbol{G}} \tag{4}$$

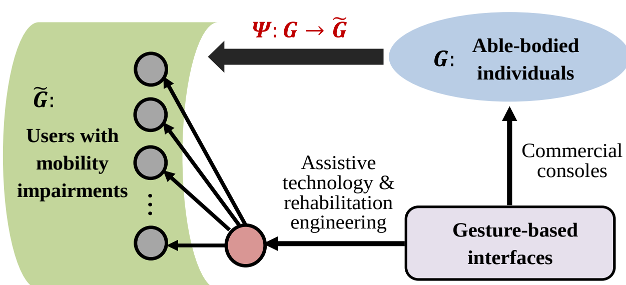

Figure 2. Problem Definition

B. Constrained Gesture Generation

An analytic approach consisting four steps was presented in our previous work to solve the problem by converting an existing gesture-based interface designed for individuals without disabilities to be usable by individuals with upper motor impairments: (1) gesture trajectory acquisition and preprocessing; (2) feature extraction; (3) transformation; and (4) gesture generation.

The first step collected two sets of gesture instances through interviews with able-bodied subjects and subjects with quadriplegia, respectively. The recorded trajectories were preprocessed to remove outliers and smoothed. In step (2), a K dimensional feature vector (including Laban space, Kinematic, and Geometric features) was extracted from each gesture instance. Step (3) computed a transform function for each training gesture using regression trees [22]. In step (4), for each testing gesture, an iterative process with two steps was used to generate a candidate set using the pre-trained transform function and a gesture generator.

Through the four-step process, a candidate gesture set was obtained for each testing gesture. A subjective approach was then applied to select the final gesture set [21]. While reported selected gestures complied with the user in terms of the total effort and preference, they may not be stable (in the sense of control) when they are in practical use. The current work addressed this issue.

III. Methodology

A stability-based filter employing UCM framework is used to acquire the variability for each gesture in the candidate set. The goal is to pick those gestures that allow for the largest redundancy of the motor system to construct the final gesture set $\widetilde{\boldsymbol{G}}$. This filter is applied to identify differences in stability in joint configuration space for different gestures.

A. System Architecture

The architecture of the proposed system is illustrated in Figure 1. The final gesture set is determined through a five-step procedure: (a) modeling constrained human arm system; (b) recording and pre-processing the skeleton data using Kinect sensor; (c) computing variability and stability indices for constrained candidate gestures based on UCM framework; (d) simulating the gestures using a WAM robotic arm and evaluating gestures based on an empiric metric (*work*); (e) determining the final gesture set based on an integration of stability and *work*.

B. Constrained Human Arm System Model

The Kinematic chain of a human arm system is modeled as in Figure 3. Shoulder, elbow, and wrist joint's configuration are denoted as control variables. The target users of our system (individuals with Cervical 1 to Cervical 8 quadriplegia) are lack of hands and wrists function. Thus, the constrained human arm model ignores the wrist joint's orientation. The DOF for the joint space (denoted as R) is four: 3DOF for the shoulder and 1DOF for the elbow. The DOF of task space (denoted as d) is three. Therefore, the constrained human arm system (with $R > d$) is redundant.

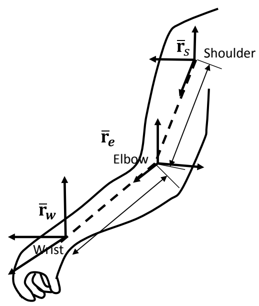

Figure 3. Schematic of a constrained human arm system

Let $\boldsymbol{r_s}$, $\boldsymbol{r_e}$, and $\boldsymbol{r_w}$ denote the 3D coordinates of the shoulder, elbow, and wrist joint, which are acquired from Kinect sensor. The coordinate system of Kinect is illustrated as in Figure 4, and the Kinect sensor is used to obtain the human skeleton information from the images acquired.

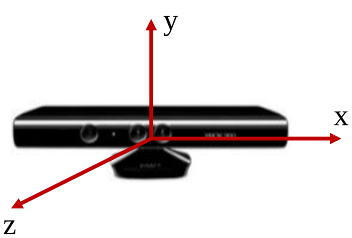

Figure 4. Kinect coordinate system

The approach presented by Nisky [16] is applied to represent the 3D task space using shoulder and elbow joints' configurations. The constrained human arm system and Kinect's coordinate system is registered as illustrated in Figure 5. Here, α_s and α_e represent the absolute horizontal angles of the joints, while β_s and β_e are the absolute vertical angles of the joints. Then, the joint configurations of the arm (denoted as θ) at the kth frame is expressed as $\theta(k) = [\alpha_s, \alpha_e, \beta_s, \beta_e]^T$.

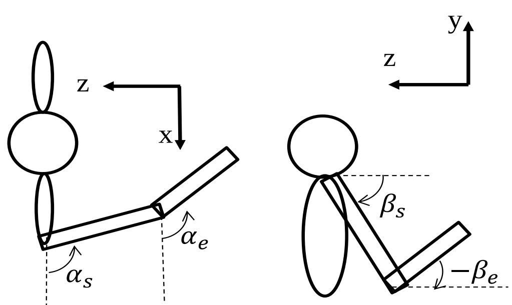

Figure 5. Task space representation vs. control variables for constrained human arm system

C. Data Collection and Processing

A three-step pre-processing procedure is conducted to reduce noise and smooth the shoulder, elbow, and hand trajectories: (1) outlier removal; (2) Butterworth filter; and (3) Kalman filter. An outlier is defined as a point that lies far from the mean of all the points (of a gesture instance) on the trajectory. This distance is measured with respect to the standard deviation. The points with a larger distance than three times the standard deviation from the mean value are discarded. Due to sensor noise and measurement errors, spatial trajectories are never accurate. In this work, a Butterworth filter together with a Kalman smoothing filter is employed to smooth the 3D trajectories. Moreover, to apply UCM through all gesture instances, $\boldsymbol{r_s}(k)$, $\boldsymbol{r_e}(k)$ and $\boldsymbol{r_w}(k)$ are normalized through time frame.

For each gesture instance, the average center of the shoulder is computed and treated as the origin of the human arm coordinate system. Then, the end effector's (hand's) 3D coordinate (denoted as $\boldsymbol{X}(k)$) is represented as $\boldsymbol{X}(k) = [x(k), y(k), z(k)]^T$, where $\boldsymbol{X}(k)$ is obtained using $\boldsymbol{r_s}(k)$ and $\boldsymbol{r_w}(k)$ (Eq. 5).

$$\boldsymbol{X}(k) = \boldsymbol{r_w}(k) - \boldsymbol{r_s}(k) \tag{5}$$

D. Compute the Variability using UCM

For the constrained human arm system (Figure 3), the relationship between the task and joint variables can be defined as Eq. 6. Let T denotes the number of points collected from skeleton data. The length of the upper and lower arm can be represented as L_{se} (Eq. 7) and L_{ew} (Eq. 8), respectively.

$$\boldsymbol{X}(k) = f(\boldsymbol{\theta}(k)) \tag{6}$$

$$L_{se} = \frac{1}{T}\sum_{k=1}^{T} \|\boldsymbol{r_s}(k) - \boldsymbol{r_e}(k)\| \tag{7}$$

$$L_{ew} = \frac{1}{T}\sum_{k=1}^{T} \|\boldsymbol{r_e}(k) - \boldsymbol{r_w}(k)\| \tag{8}$$

Using the method in [16], the relationship between the task and joint variables is expressed as in Eq. 9, where $c\cdot$ and $s\cdot$ are short for $\cos(\cdot)$ and $\sin(\cdot)$, respectively.

$$f(\boldsymbol{\theta}(k)) = \begin{pmatrix} x(k) \\ y(k) \\ z(k) \end{pmatrix} = \begin{pmatrix} L_{se}c\alpha_s c\beta_s + L_{ew}c\alpha_e c\beta_e \\ -L_{se}s\beta_s - L_{ew}s\beta_e \\ -L_{se}s\alpha_s c\beta_s - L_{ew}s\alpha_e c\beta_e \end{pmatrix} \tag{9}$$

Solutions for Eq. 6 are obtained from the geometrical model of the arm using a nonlinear forward kinematics equation [23]. A linear approximation around the mean joint configuration at frame k is given by Eq. 10:

$$\boldsymbol{X}(k) - \overline{\boldsymbol{X}}(k) = \boldsymbol{J}(\overline{\boldsymbol{\theta}}(k))(\boldsymbol{\theta}(k) - \overline{\boldsymbol{\theta}}(k)) \tag{10}$$

where $\boldsymbol{\theta}(k)$ and $\boldsymbol{X}(k)$ are the joints' configuration and hands' position of mth trial at frame k, $\overline{\boldsymbol{\theta}}(k)$ and $\overline{\boldsymbol{X}}(k)$ are the mean value of the joints' configuration and hands' position at frame k through all the trials, and $\boldsymbol{J}(\overline{\boldsymbol{\theta}}(k)) \in \mathbb{R}^{dXR}$ is the Jacobian matrix obtained at the mean configuration. From Eq. 9, the Jacobian can be obtained as Eq. 11.

$$J\left(\bar{\boldsymbol{\theta}}(k)\right) = \\ = \begin{pmatrix} -L_{se}s\alpha_s c\beta_s & -L_{ew}s\alpha_e c\beta_e & -L_{se}c\alpha_s s\beta_s & -L_{ew}c\alpha_e s\beta_e \\ 0 & 0 & -L_{se}c\beta_s & -L_{ew}c\beta_e \\ -L_{se}c\alpha_s c\beta_s & -L_{ew}c\alpha_e c\beta_e & L_{se}s\alpha_s s\beta_s & L_{ew}s\alpha_e s\beta_e \end{pmatrix} \quad (11)$$

At each time frame k, the deviation of the joint configuration is divided into two components: the component that does not affect the task variable (lies within the UCM) and a perpendicular component affecting the task variable (perpendicular to the UCM). The UCM can be approximated linearly by the null-space of the Jacobian matrix. The normalized basic vector of this null space (denoted as $\epsilon(k)$) is obtained using Eq. 12, with dimensionality $R-d=1$ ($\epsilon(k) \in \mathbb{R}^{RX1}$).

$$J\left(\bar{\boldsymbol{\theta}}(k)\right) \cdot \epsilon(k) = 0 \quad (12)$$

Based on the UCM framework, for the mth trial at time k, the joint variability that lies within is denoted as Eq. 13:

$$\Theta_{m||} = \sum_{i=1}^{R} [\epsilon^T(k,i) \cdot (\boldsymbol{\theta}(k) - \bar{\boldsymbol{\theta}}(k))] \cdot \epsilon(k,i) \quad (13)$$

The vector component of the joint variability lying outside the UCM is the difference between the joint variability vector and the vector component of the joint variability that lies within the UCM as Eq. 14:

$$\Theta_{m\perp} = (\theta - \bar{\theta}) - \Theta_{n||} \quad (14)$$

The variability per DOF within UCM is estimated as Eq. 15:

$$\sigma_{||}^2 = (R-d)^{-1} \cdot N_{trials}^{-1} \cdot \sum \Theta_{n||}^2 \quad (15)$$

where N_{trails} is the number of trials. Similarly, the variability per DOF outside UCM is estimated as Eq. 16:

$$\sigma_{\perp}^2 = d^{-1} \cdot N_{trials}^{-1} \cdot \sum \Theta_{\perp}^2 \quad (16)$$

The ratio between the two standard deviations is used to measure the level of stability of the trajectories in the task and user space, which in turn is associated with a particular gesture (Eq. 17). If $\sigma_{||} > \sigma_{\perp}$ ($R_V > 1$), it means that the variation of joint configurations doesn't affect the control of the task variables.

$$R_V = \frac{\sigma_{||}}{\sigma_{\perp}} \quad (17)$$

This index is applied to evaluate the stability of each constrained gesture. The goal is to find the gestures with the highest R_V values, which encode high stability (highly redundant).

E. Candidate Gestures

Figure 6 illustrates a standard gesture set designed for a commercial gesture console. In our previous work [21], applying the analytic approach described in section III, seventeen constrained candidate gestures (Figure 7) were obtained for each standard gesture in Figure 6.

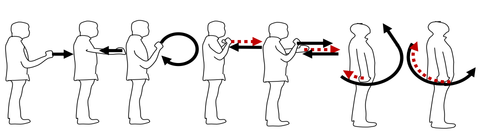

(a) (b) (c) (d) (e) (f) (g)

Figure 6. Standard gesture set

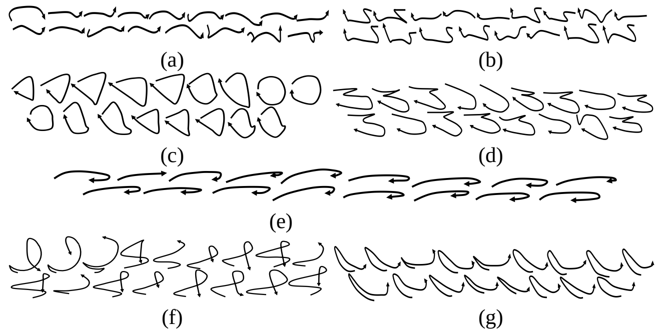

Figure 7. Constrained candidate gestures set

IV. Experimental Results

A. Determine an Accessible Gesture Set Based on UCM

Two male subjects with quadriplegia due to Cervical 5 (C5) to Cervical 6 (C6) spinal cord injury (SCI) were recruited in the experiment. The experiment's procedure was approved by Purdue Institutional Review Board (IRB) and Rehabilitation Hospital of Indianapolis (RHI). The condition for inclusion to the experiments was subjects with quadriplegia due to C1 to C8 SCI. During the experiment, the subjects were asked to perform each gesture (Figure 6 and 7, respectively) for five trials following the trajectories shown on PowerPoint slides. A Kinect sensor was used to record the data associated with the subjects' skeleton motion during the gesture performance. The experiments were conducted with the subjects at the InterFACE lab in RHI with the setting illustrated as in Figure 8.

Figure 8. Setting for the experiment

To determine an accessible gesture set, the stability index (Eq. 17) was computed for the standard (Figure 6) and candidate gestures (Figure 7) based on the UCM method presented in Section III. D. The average stability index R_V for the standard gestures in Figure 6 (with gesture index "0") and constrained candidate gestures in Figure 7 (with gesture index "1" to "17") is illustrated as in Figure 9. The goal for the UCM based approach is to select gestures with the highest stability (the highest bar) from each candidate set. From the bar graph, the gestures with the largest stability index were "1" (Figure 9a), "4" (Figure 9b), "8" (Figure 9c), "5" (Figure 9d), "2" (Figure 9e), "12" (Figure 9f), and "12" (Figure 9g), respectively. The corresponding average stability indexes were 2.001, 1.887, 1.613, 1.377, 1.804, 1.720, and 0.978. The results revealed that all the selected gestures (with the highest stability) were from constrained candidate gesture set. This result was consistent with the subjective gesture selection method in [21] and validated the analytic gesture generation approach presented in [21]. The selected component for the accessible gesture set is shown as in Figure 10.

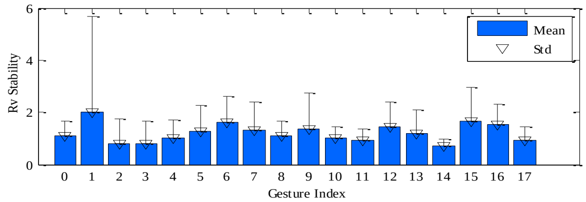

(a) Stability for gestures in Figure 7 (a)

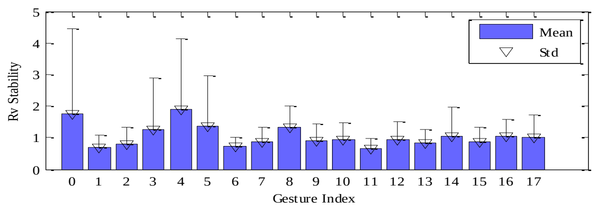

(b) Stability for gestures in Figure 7 (b)

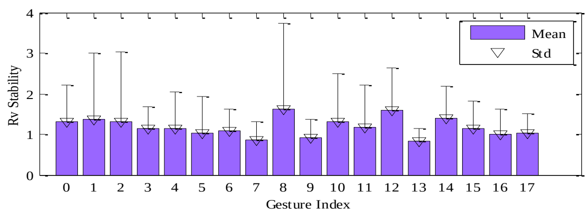

(c) Stability for gestures in Figure 7 (c)

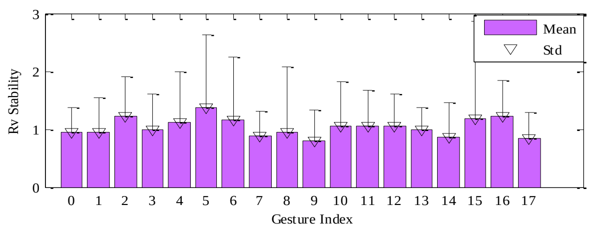

(d) Stability for gestures in Figure 7 (d)

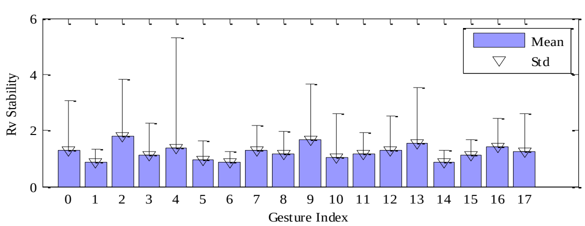

(e) Stability for gestures in Figure 7 (e)

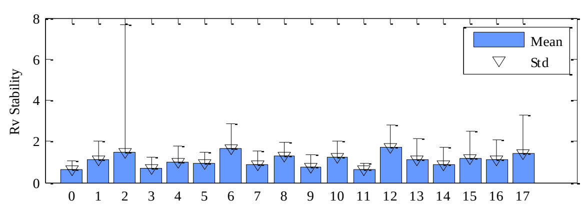

(f) Stability for gestures in Figure 7 (f)

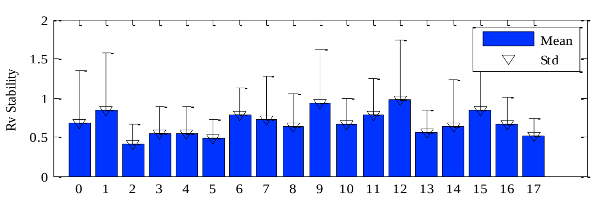

(g) Stability for gestures in Figure 7 (g)

Figure 9. Average stability indexes for the standard and constrained gestures

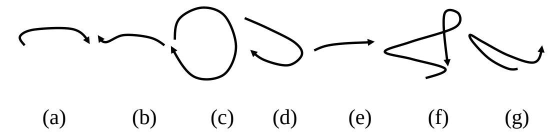

Figure 10. The selected gesture set based on UCM method

B. *Gesture Selection using WAM Robotic Arm*

In this section, the human arm system is approximated by a 7 DOF WAM robotic arm. The main assumption leading this part of the research is that the effort required to complete a gesture can be approximated by the *Work* exhorted by a robot. The WAM arm is used to perform each standard and constrained gesture trajectory for five trials. Figure 11 is an illustration of the WAM arm performing a constrained gesture trajectory.

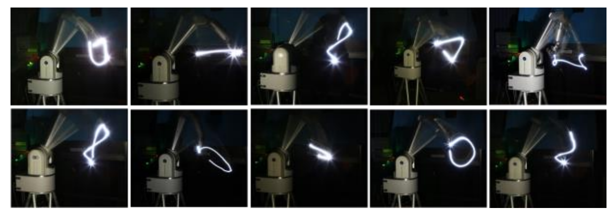

Figure 11. Constrained gestures performed by a WAM arm (laser light traces were used to highlight the trajectories)

The torque (denoted as τ) and angles (denoted as θ) for each joint is recorded. The total *Work* (Eq. 18) for each gesture trajectory is computed and used as an assessment of effort required to complete that gesture. The gesture with the least effort is selected to narrow down the candidate gestures to the final accessible gesture set.

$$W = \int_{\theta_1}^{\theta_2} \tau \, d\theta \qquad (18)$$

Where, the variables θ_1 and θ_2 are the joint configuration at time frame t and $t+1$, respectively. τ is the average torque during time frame t and $t+1$.

C. *Integration between Stability and Work objective indices*

Integration was made between stability and work indices to determine the accessible gesture set. Let S_i $(i = 1,2,\ldots,N)$ denote a set of gestures that have highest α_i percentile of stability and W_i denote a set of gestures that have the lowest α_i percentile of *work*. The integration method consisted of increasing α_i iteratively by small increments until the intersection between the two sets is exactly one gesture ($|S_i \cap W_i| = 1$). The α_i% value found for each gesture class were 26.3%, 0% (gesture with the highest stability and lowest work was selected), 2.1%, 30.9%, 0%, 20.7%, and 22.6%, respectively.

From the results, the indices of constrained gestures found by the integration method were “15”, “4”, “12”, “5”, “2”, “2”, and “9”, respectively (Figure 12). The final result is a vocabulary of a single gesture per class.

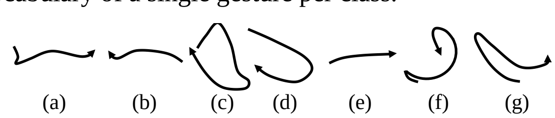

Figure 12. The selected gesture set using the integration method

V. Conclusion and Future Work

This paper presented one approach to find sets of accessible gestures that can be used by users with physical disabilities to interact with computing devices as an alternative to standard gesture sets commonly found in gaming consoles. The UCM method analyzed the variability and stability of human motion when they were performing the gestures. The stability indices were then computed to determine the optimality of the gestures in the candidate set. Later, the gestures were executed in practice by a WAM robotic arm, mimicking each gesture trajectory. Objective metrics were found through this physical implementation linking the human physical motion and those of the robot. Once the stability and physical indices were obtained from the UCM method and the WAM arm, an integration was made to determine the final accessible gesture set.

We learned that two out of seven gestures found by the UCM method agreed (with the highest stability and lowest work) with the results obtained from the robotic arm (Figure 10 and 12 b, e). In addition, one gesture (Figure 12 d) found by the integration method was the same as that (Figure 10 d) obtained from the UCM method. For all the gesture classes, the accessible gestures found were within 30.9% of the optimality of stability and work, respectively. These results indicated that the gestures found by the integration method incorporate the factors of subjects' motion stability together with objective physical matrices. Moreover, it revealed that the robotic arm can be used as a tool to approximate the human arm system and complement the lack of subjects. It is effective for prototyping and designing gesture sets for able-bodied users and subjects with disabilities.

Future work will include: 1) expanding the experiments to recruit more quadriplegic subjects due to C-1 to C-8 level of SCI; 2) evaluating the effectiveness of the constrained gestures by recruiting subjects with quadriplegia to perform navigational tasks that can serve also as rehabilitation therapy.

References

[1] G. R. S. Murthy and R. S. Jadon, "A review of vision based hand gestures recognition," *Int. J. Inf. Technol. Knowl. Manag.*, vol. 2, no. 2, pp. 405–410, 2009.

[2] F. Adib, "Electrical muscle stimulator," US8630713 B2, 14-Jan-2014.

[3] G. Alankus, "Motion-Based Video Games for Stroke Rehabilitation with Reduced Compensatory Motions," *Electron. Theses Diss.*, Jan. 2011.

[4] W. Akram, L. Tiberii, and M. Betke, "A Customizable Camera-Based Human Computer Interaction System Allowing People with Disabilities Autonomous Hands-Free Navigation of Multiple Computing Tasks," in *Universal Access in Ambient Intelligence Environments*, C. Stephanidis and M. Pieper, Eds. Springer Berlin Heidelberg, 2007, pp. 28–42.

[5] S. C. Lee, B. Li, and T. Starner, "AirTouch: Synchronizing In-air Hand Gesture and On-body Tactile Feedback to Augment Mobile Gesture Interaction," in *2011 15th Annual International Symposium on Wearable Computers (ISWC)*, 2011, pp. 3–10.

[6] J. Cassell, "A Framework For Gesture Generation And Interpretation," in *Computer Vision in Human-Machine Interaction*, 1998, pp. 191–215.

[7] H. Jiang, J. P. Wachs, and B. S. Duerstock, "Facilitated Gesture Recognition Based Interfaces for People with Upper Extremity Physical Impairments," in *Progress in Pattern Recognition, Image Analysis, Computer Vision, and Applications*, L. Alvarez, M. Mejail, L. Gomez, and J. Jacobo, Eds. Springer Berlin Heidelberg, 2012, pp. 228–235.

[8] M. Nielsen, M. Störring, T. B. Moeslund, and E. Granum, "A Procedure for Developing Intuitive and Ergonomic Gesture Interfaces for HCI," in *Gesture-Based Communication in Human-Computer Interaction*, A. Camurri and G. Volpe, Eds. Springer Berlin Heidelberg, 2004, pp. 409–420.

[9] S. Padam Priyal and P. K. Bora, "A robust static hand gesture recognition system using geometry based normalizations and Krawtchouk moments," *Pattern Recognit.*, vol. 46, no. 8, pp. 2202–2219, Aug. 2013.

[10] H. Jiang, B. S. Duerstock, and J. P. Wachs, "A Machine Vision-Based Gestural Interface for People With Upper Extremity Physical Impairments," *IEEE Trans. Syst. Man Cybern. Syst.*, vol. 44, no. 5, pp. 630–641, May 2014.

[11] J. Zeng, Y. Sun, and F. Wang, "A Natural Hand Gesture System for Intelligent Human-Computer Interaction and Medical Assistance," in *2012 Third Global Congress on Intelligent Systems (GCIS)*, 2012, pp. 382–385.

[12] J. P. Wachs, "Optimal Hand Gesture Vocabulary Design Methodology for Virtual Robotic Control." Doctoral dissertation, Ben-Gurion University of the Negev, 2006.

[13] A. Pereira, J. P. Wachs, K. Park, and D. Rempel, "A User-Developed 3-D Hand Gesture Set for Human–Computer Interaction," *Hum. Factors J. Hum. Factors Ergon. Soc.*, p. 0018720814559307, Nov. 2014.

[14] J. Grosek and J. N. Kutz, "Selecting a Small Set of Optimal Gestures from an Extensive Lexicon," *ArXiv14047594 Cs*, Apr. 2014.

[15] K. Davids, S. Bennett, and K. M. Newell, *Movement System Variability*. Human Kinetics, 2006.

[16] I. Nisky, M. H. Hsieh, and A. M. Okamura, "A framework for analysis of surgeon arm posture variability in robot-assisted surgery," in *2013 IEEE International Conference on Robotics and Automation (ICRA)*, 2013, pp. 245–251.

[17] J. P. Scholz and G. Schöner, "The uncontrolled manifold concept: identifying control variables for a functional task," *Exp. Brain Res.*, vol. 126, no. 3, pp. 289–306, May 1999.

[18] V. Martin, "A dynamical systems account of the uncontrolled manifold and motor equivalence in human pointing movements," Bochum University, 2005.

[19] I. Nisky, M. Hsieh, and A. Okamura, "Uncontrolled manifold analysis of arm joint angle variability during robotic teleoperation and freehand movement of surgeons and novices," *IEEE Trans. Biomed. Eng.*, Jun. 2014.

[20] M. L. Latash, J. P. Scholz, F. Danion, and G. Schoner, "Motor Control Strategies Revealed in the Structure of Motor... : Exercise and Sport Sciences Reviews." [Online]. Available: http://journals.lww.com/acsmessr/Fulltext/2002/01000/Motor_Control_Strategies_Revealed_in_the_Structure.6.aspx.

[21] H. Jiang, B. S. Duerstock, and J. P. Wachs, "An Analytic Approach to Decipher Usable Gestures for Quadriplegic Users," presented at the *2014 IEEE International Conference on Systems, Man and Cybernetics*, San Diego, CA, USA, 2014.

[22] G. De'ath and K. E. Fabricius, "Classification and Regression Trees: A Powerful yet Simple Technique for Ecological Data Analysis," *Ecology*, vol. 81, no. 11, pp. 3178–3192, Nov. 2000.

[23] J.-P. Merlet, "Solving the Forward Kinematics of a Gough-Type Parallel Manipulator with Interval Analysis," *Int. J. Robot. Res.*, vol. 23, no. 3, pp. 221–235, Mar. 2004.